Supporting Information

Phosphorus doping stabilized $LiNi_{0.83}Co_{0.12}Mn_{0.05}O_2$ with enhanced elevated temperature electrochemical performance for Li-ion battery

Xin Wang, Xiaoyu Zhang, Fangyuan Cheng, Peng Wei, Qi Li, Jia Xu, Qing Li, Yue Xu, Shixiong Sun, Chun Fang*, Jiantao Han*

State Key Laboratory of Material Processing and Die & Mould Technology, School of Materials Science and Engineering, Huazhong University of Science and Technology, Wuhan, Hubei 430074, China

Corresponding author

* E-mail addresses: fangchun@hust.edu.cn (C. Fang)

jthan@hust.edu.cn (J.T. Han).

Author Contributions

X.W did the main work and others provided important help.

Additional computational details

1. The time to break a P-O bond of PO_4^{3-}.

The Vienna Ab Initio Package (VASP)[1,2] was employed to perform all the spin-polarized density functional theory (DFT) calculations within the generalized gradient approximation (GGA) using the PBE formulation.[3] The projected augmented wave (PAW) potentials[4,5] was chosen to describe the ionic cores and take valence electrons into account using a plane wave basis set with a kinetic energy cutoff of 400 eV. The correction function Grimme is used to correct the van der Waals force (vdW) dispersion interaction.[6] Partial occupancies of the Kohn-Sham orbitals were allowed using the Gaussian smearing method and a width of 0.1 eV. The electronic energy was considered self - consistent when the energy change was smaller than 10^{-6} eV. A geometry optimization was considered convergent when the force imposed on each atom was smaller than 0.01 eV、Å。The atomic vibration frequencies were calculated via the finite displacement methods.[7] The CINEB methods[8] were used to calculate the energies of the transition states during P - O bond breaking.

The structure of PO_4^{3-} located in the supercell of 30.09 Å *18.09 Å *18.09 Å were optimized. The k - points were set as 1×2×2 with the M - P sampling methods. All the bond lengths of P-O were about 1.56 Å and all the bond angles of P-O-P were about 109.5°

The time to break a P-O bond is defined as follow:

$$t = \frac{1}{v_0} exp(E_a / k_B T)$$

where v_0 is the vibration frequency of the O atom, E_a is the energy barrier corresponding to the P-O bond breaking, k_B is the Boltzmann constant, and T is the temperature.

The O atom vibration frequencies of the Longitudinal wave and two transverse waves are 2.30E13Hz, 6.74E12Hz and 6.58E12Hz, respectively. The vibration direction of the Longitudinal wave is along the P-O bond, which is responsible for the P-O bond breaking. Therefore, the vibration frequencies of the Longitudinal wave 2.30E13Hz was used to calculate the time to break a P-O bond of PO_4^{3-}.

2. Doping sites of P atoms.

Partial occupancies of the Kohn-Sham orbitals were allowed using the Gaussian smearing method and a width of 0.05 eV. The electronic energy was considered self-consistent when the energy change was smaller than 10^{-5} eV. A geometry optimization was considered convergent when the force change was smaller than 0.02 eV / Å. Grimme's DFT-D3 methodology was used to describe the dispersion interactions.

The equilibrium lattice constants of hexagonal $LiNiO_2$ unit cell (model 0) were optimized, when using a 15×15×3 Monkhorst-Pack k-point grid for Brillouin zone sampling, to be a=b=2.831 Å, c=13.824 Å. Then it was used to construct a $LiNiO_2$ supercell with 3×3×1 periodicity. It comprises of 27 Li, 27 Ni and 54 O atoms. During structural optimizations, the Γ point in the Brillouin zone was used for k-point sampling, and all

atoms were allowed to fully relax.

3. The formation energy of oxygen vacancy.

The formation energy of oxygen vacancy was calculated by the following formula:

$\Delta E_{form}(Vo) = E(defect) - E\ (perfect) + 1/2Egas(O_2)$

Where the $\Delta E_{form}(Vo)$, E(defect), E (perfect), $Egas(O_2)$ represents formation energy of oxygen vacancy, the total energy of bulk with and without oxygen vacancy, and the energy of O_2 molecule in the gas phase, respectively.

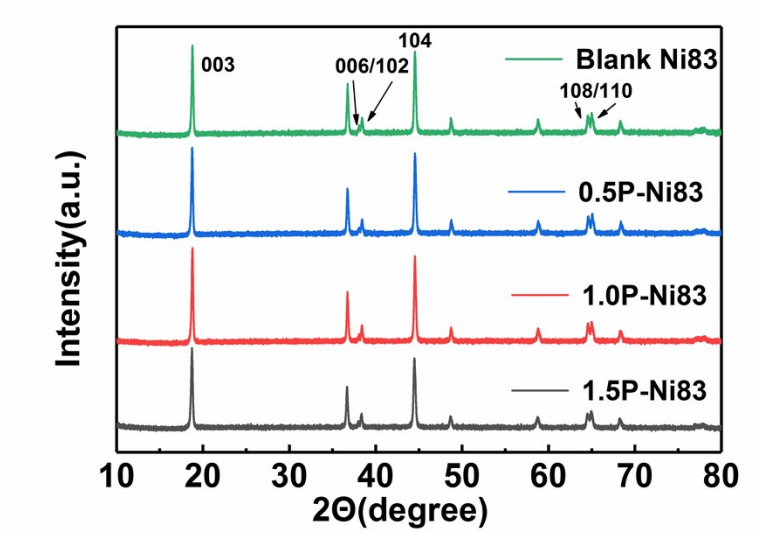

Figure S1. XRD patterns of Blank Ni83, 0.5P-Ni83, 1.0P-Ni83 and 1.5P-Ni83 cathodes.

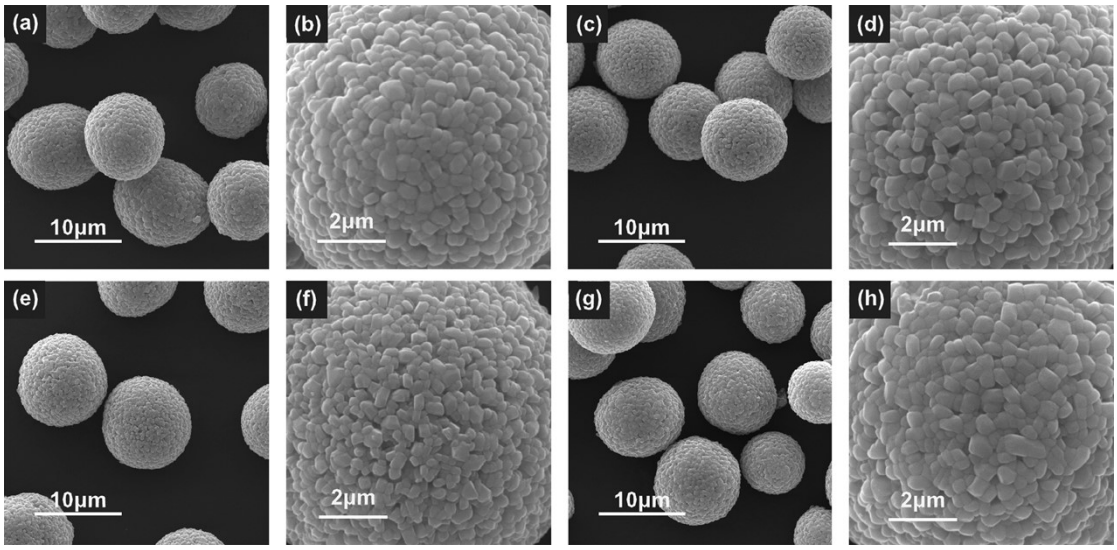

Figure S2. The SEM images of a, b) Blank Ni83, c, d) 0.5P-Ni83, e, f) 1.0P-Ni83 and g, h) 1.5P-Ni83.

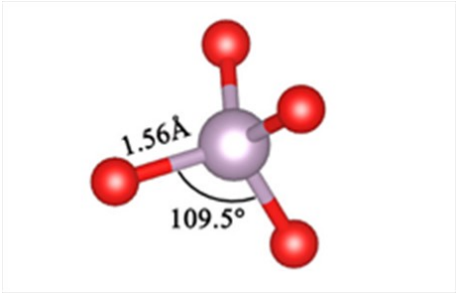

Figure S3 The structures of PO_4^{3-}.

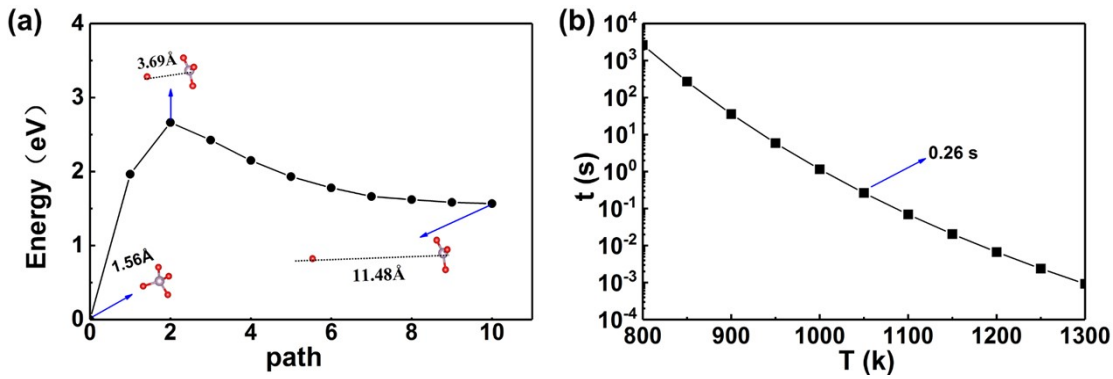

Figure S4 a) The energy barrier corresponding to the P-O bond breaking of PO_4^{3-}. b) The time to break a P-O bond of PO_4^{3-} vs. the temperature.

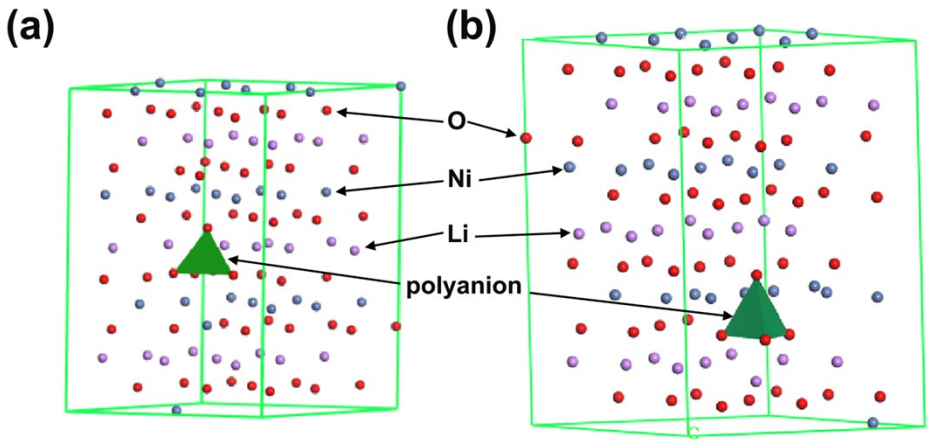

Figure S5 a) model 1: P in Li layer. b) model 2: P in Ni layer.

Table S1 Calculation results of different model energy.

gas molecules		model 0: pristine			model 1: P in Li layer		
molecule	E_{tot} (eV)	model	E_{tot} (eV)	$E_{f, Ovac}$ (eV)	model	E_{tot} (eV)	$E_{f, Ovac}$ (eV)
O_2(g)	-9.852	*	-628.508		*	-635.100	
		[with 1 O_{vac}]	-621.796	1.79	[with 1 O_{vac}]	-627.404	2.77

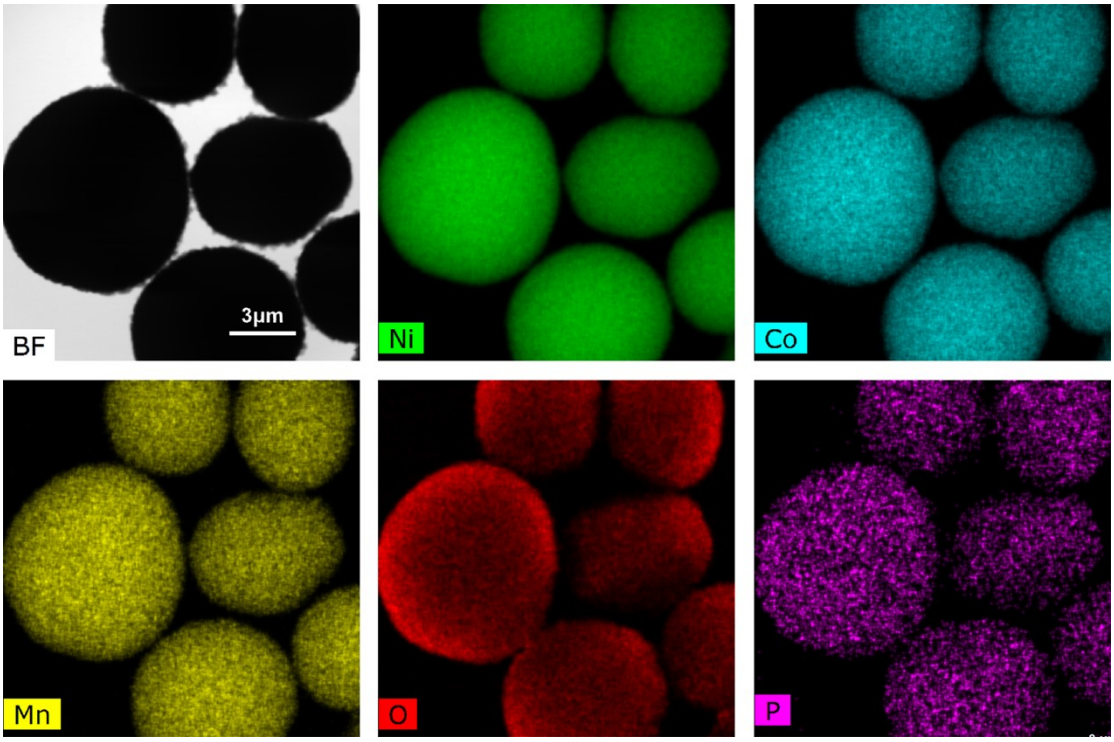

Figure S6. EDS mapping of Ni, Co, Mn, O and P of 1.0P-Ni83.

Table S2. Element composition of the bulk particles for Blank Ni83 and 1.0P-Ni83 by ICP-AES.

Sample	Li (mol%)	Ni (mol%)	Co (mol%)	Mn (mol%)	P (mol%)
Blank Ni83	102.021	83.004	12.314	4.681	0
1.0P-Ni83	102.700	83.019	12.337	4.641	0.813

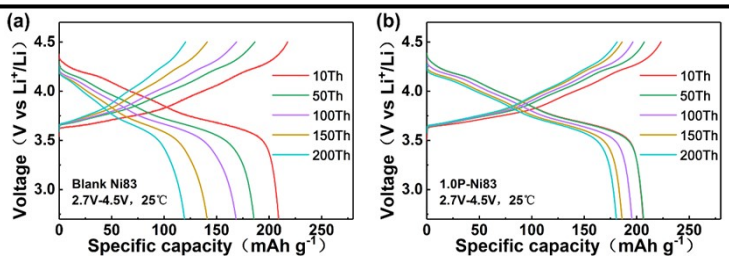

Figure S7. a, b) Typical charge-discharge profiles of Blank Ni83 and 1.0P-Ni83 between 2.7-4.5 V at 25 °C.

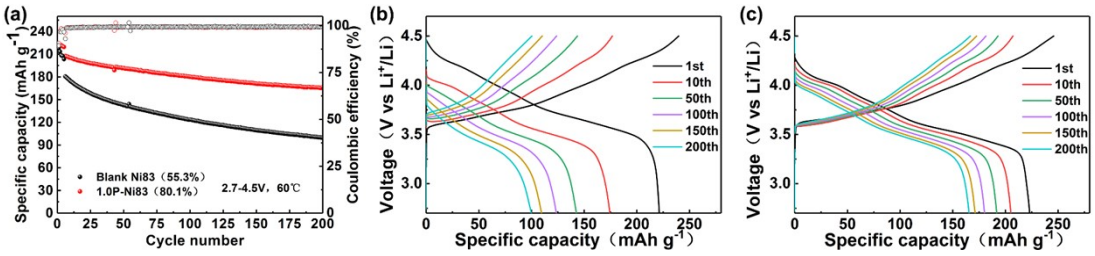

Figure S8. a) Cycle performance between 2.7-4.5 V at 60 °C of Blank Ni83 and 1.0P-Ni83. b, c) Typical charge-discharge profiles of Blank Ni83 and 1.0P-Ni83 between 2.7-4.5 V at 60 °C.

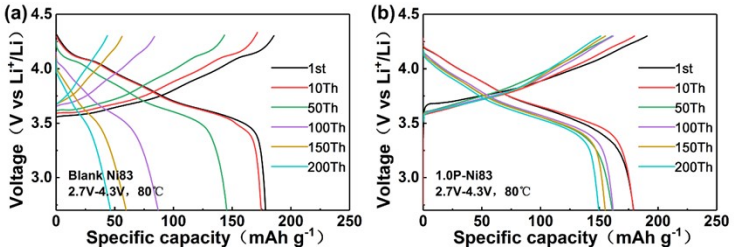

Figure S9. a, b) Typical charge-discharge profiles of Blank Ni83 and 1.0P-Ni83 between 2.7-4.3 V at 80 °C.

Table S3. Electrochemical performance comparison for Blank Ni83 and 1.0P-Ni83.

	2.7-4.5 V, 25 °C		2.7-4.3 V, 60 °C		2.7-4.5 V, 60 °C		2.7-4.3 V, 80 °C	
Sample	Capacity at 1C (mAh g^{-1})	200Cs retention	Capacity at 1C (mAh g^{-1})	500Cs retention	Capacity at 1C (mAh g^{-1})	200Cs retention	Capacity at 1C (mAh g^{-1})	200Cs retention
Blank Ni83	202	52.4%	179	21.4%	182	55.3%	180	11.4%
1.0P-Ni83	197	88.3%	180	80.2%	208	80.1%	178	84.7%

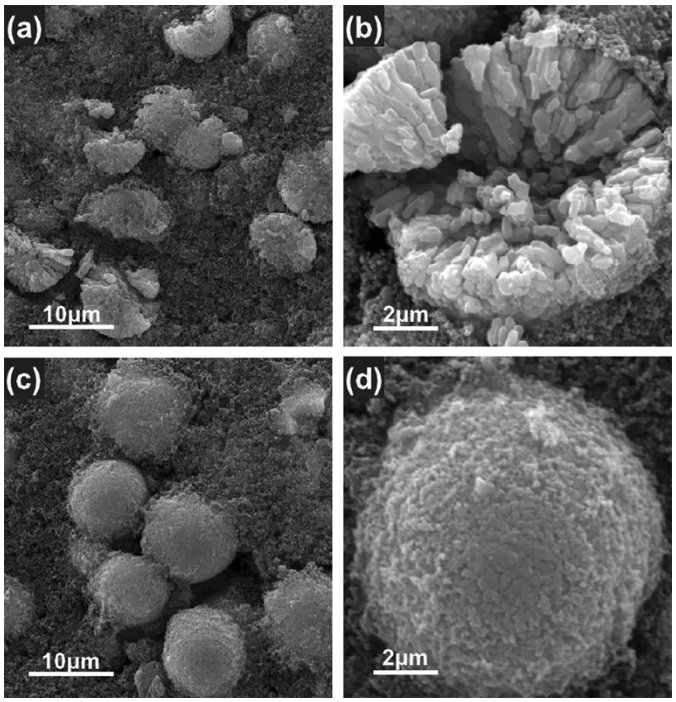

Figure S10. SEM images after 200 cycles between 2.7-4.3 V at 60 °C of a, b) Blank Ni83 electrode c, d) 1.0P-Ni83 electrode.

Table S4. The fitted impedance parameters of equivalent circuits.

Cycle	R_f/ohm		R_{ct}/ohm	
	Blank Ni83	1.0P-Ni83	Blank Ni83	1.0P-Ni83
Fresh	--	--	25.64	24.83
50th	65.99	55.72	227.20	86.04
100th	154.90	63.39	648.10	140.40

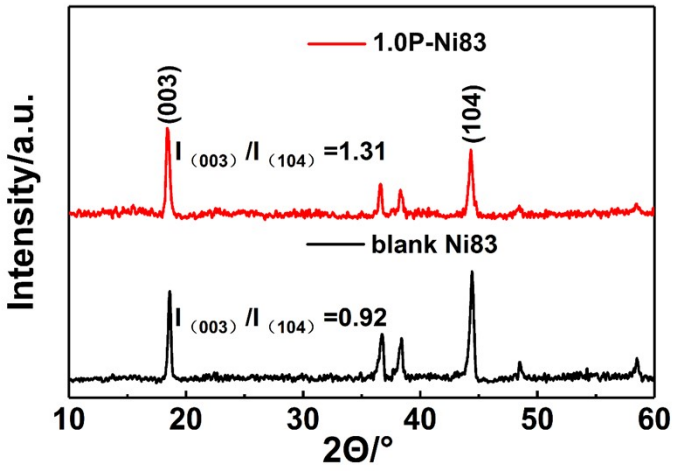

Figure S11. XRD patterns after 200 cycles between 2.7-4.3 V at 60 °C of Blank Ni83 electrode and 1.0P-Ni83 electrode.

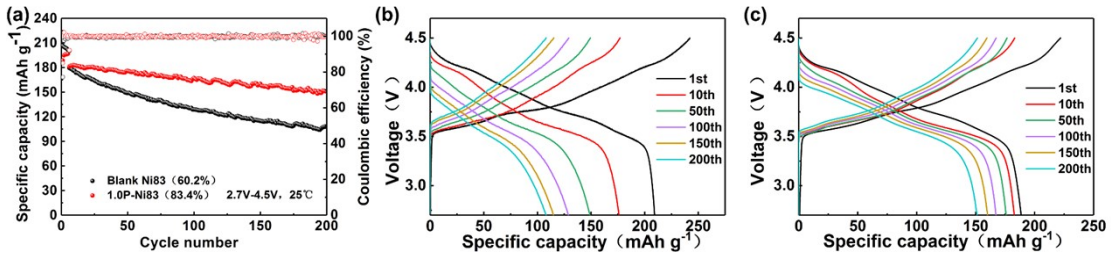

Figure S12. a) Cycling performance of full cell for Blank Ni83 and1.0P-Ni83 at 1 C between 2.7-4.5 V at 25 °C. b, c) Typical charge-discharge profiles of full cell for Blank Ni83 and 1.0P-Ni83 between 2.7-4.5 V at 25 °C.

References

[1] Kresse, G.; Furthmüller, Comput. Mater. Sci. 1996, 6, 15-50, doi:10.1016/0927-0256(96)00008-0.

[2] Kresse, G.; Furthmüller, Phys. Rev. B 1996, 54, 11169−11186, doi:10.1103/PhysRevB.54.11169.

[3] Perdew, J. P.; Burke, K.; Ernzerhof, Phys. Rev. Lett. 1996, 77, 3865-3868,

doi:10.1103/PhysRevLett.77.3865.

[4] Kresse, G.; Joubert, D. Phys. Rev. B 1999, 59, 1758-1775, doi:10.1103/PhysRevB.59.1758.

[5] Blöchl, P. E. Phys. Rev. B 1994, 50, 17953-17979, doi:10.1103/PhysRevB.50.17953.

[6] E.R. McNellis, J. Meyer, K. Reuter, Phys. Rev. B 80 (2009), doi:10.1103/PhysRevB.80.205414.

[7] Parlinski K, Li Z Q, Kawazoe Y. Physical Review Letters, 1997, 78(21): 4063, doi:10.1103/PhysRevLett.78.4063.

[8] Henkelman G, Uberuaga B P, Jónsson H. The Journal of chemical physics, 2000, 113(22): 9901-9904, doi:10.1063/1.1329672.